

INFLUENCE OF VARIOUS GEOMETRIES ON DETECTION EFFICIENCY OF POLYSTYRENE, POLYVINYL-TOLUENE, AND SODIUM IODIDE DETECTORS USING GEANT4

by

Sikander M. MIRZA, Ahsan RAZZAQ, Shakeel Ur REHMAN, and Nasir M. MIRZA*

Department of Physics and Applied Mathematics, Pakistan Institute of Engineering and Applied Sciences, Islamabad, Pakistan

Scientific paper

DOI: 10.2298/NTRP1503188M

In this work, comparative study on energy dependence of absorbed, intrinsic, photo-peak and absolute total efficiency of polystyrene plastic scintillation fiber and polyvinyl-toluene detectors with NaI(Tl) scintillation detectors has been performed using Geant4 version 9.6 toolkit. The effects of geometry parameters on various efficiencies were investigated by varying detector radii, thickness and various source-to-detector configurations. These studies were carried out for both cylindrical and slab geometries for photon energy range of 10 keV-20 MeV using point isotropic sources and parallel beams of photons. Comparisons of the Geant4.9.6 based simulations for polystyrene scintillation fiber intrinsic efficiency as a function of photon energy and corresponding results obtained by earlier versions Geant4 (version 5.1) and Geant4 (version 8.1) show good agreements. The variation of the intrinsic efficiency with energy for polyvinyl-toluene is also found to match very well with respective earlier results. This work confirms that the plastic scintillator based fibers and slab detectors are suitable for X-ray and low energy γ -ray applications with energies typically below 50 keV with the optimum length of polystyrene scintillation fiber equal to 10 cm. For high energy range, cross talk remains an issue for polystyrene scintillation fiber and it is prominent in fibers having longer lengths and small diameters. Also, until the fiber radius is smaller than the incident photon beam, the fiber intrinsic efficiency increases with an increase in the radius.

Key words: plastic scintillator fiber, polyvinyl-toluene scintillator, detection efficiency, Geant4

INTRODUCTION

Recent developments in the image-guided radiotherapy by linear-accelerators and magnetic resonance imaging (MRI) integration have tremendous improvements in the accuracy of dose delivered to the patients. The advancements intensity-modulated radiotherapy and inter-operative radiotherapy have made it necessary for dosimeters to be highly accurate, reliable and should have high spatial resolution. In this regard, plastic scintillators have shown advantages over other dosimeters because they exhibit superior resolution and are resistant to the radiation damage. Also, their response remains independent of external electromagnetic field [1]. In post-accident scenarios for nuclear installations, conventional gas ionization detectors or inorganic scintillator based radiation monitors including dosimeters and tele-detectors become inadequate due to their activation. In such areas, the scintillation based optical fibers are becoming a promising candi-

date for dosimeter because they are radiation resistant and have shown linear response over the large range of radiation field strength [2].

Plastic scintillators are basically polymer based matrices belonging to polystyrene (PS), polyvinyl toluene (PVT) or poly-methyl-methacrylate (PMMA) groups. Early work on plastic scintillator fibers showed their potential as low energy photon detectors [3, 4]. Clark *et al.*, carried out experimental measurements of the intrinsic scintillation efficiency of plastic scintillators using Co-60 [5]. Later, evaluation of scintillation fiber optics as radiation imaging detectors was done by Shao *et al.*, to find basic characteristics of plastic scintillating fiber for α -particles, X-rays, γ -rays and neutrons [6]. Many researchers have also appreciated potential of these fibers as position sensitive detectors for neutrons, X- and γ -rays [7].

Plastic scintillation detectors have also shown favorable properties for dosimetry including water equivalence, fast response, high reproducibility, good flexibility, linear response above specific energy threshold, dose linearity, electromagnetic immunity, and independence

* Corresponding author; e-mail: nmm@pieas.edu.pk

of operating temperature [1]. Several experimental studies have indicated that the plastic scintillators are resistant to radiation damage [8]. Mainardi and Bonzi have shown in their Monte Carlo studies that silicon doped plastic scintillators exhibit air-equivalent behavior in energy range of interest for radiology and surface radiotherapy [9]. Due to their non-invasive nature towards prevailing radiation field, they are regarded as ideal dosimeters for quality assurance work in radiation therapy [10]. Water equivalent plastic scintillators have been developed by employing PVT as base material with 4 % chlorine as additive which yields radiological properties matching those of water within 10 % in 20 keV-662 keV energy range [11]. Recently research work has shown that conventional scintillators are not well-suitable for real time in-vivo dosimetry in brachytherapy while plastic scintillators are designed for such work [12].

The optimal signal efficiency and minimization of noise are two important considerations for clinical utilization of plastic scintillation detectors. Optimization of design optical variables was carried out by Beddar *et al.*, after minimizing Cherenkov noise and improving signal-to-noise characteristics of plastic fiber scintillators. The dependence of total absolute detection efficiency on photon energy and source-to-detector distance was studied. Also, variation of linear attenuation coefficient of detector material with photon energy was determined using MCNP code [13]. Linearity of energy response of plastic scintillators was observed above specific energy threshold. Lambert *et al.* also have shown that plastic scintillators demonstrate a linear response for high dose rate brachytherapy and have found linear increase of 100 % in dose from 50 kVp to 125 kVp energy range [12].

In order to demonstrate the usefulness of plastic scintillating fiber for X-ray imaging particularly for computerized tomography (CT) or digital radiography (DR) applications, experiments were carried out [14]. Only radio-chromatic films offered the required spatial resolution but their sensitivity remained limited and also their radiation characteristics were different from those of tissues [15]. PENELOPE [16] based Monte Carlo simulations were performed for assessment of suitability of plastic scintillators for radiation dosimetry [16] as well as Geant4 [17]. Monte Carlo simulations were performed to evaluate performance of a simple prototype X-ray detector consisting of plastic scintillating fibers connected to a charge-coupled device [18]. They found suitability of such systems for X-ray imaging in low energy range (20 keV-120 keV).

Recently Monte Carlo simulation based Geant4 toolkit was employed for estimating detection efficiency of plastic scintillating fiber using gamma rays in 0.1 MeV-10 MeV energy range by Tang *et al.* The simulation results were found in good agreement with the theoretical predictions. Later, this work was extended using Geant4 toolkit for gamma rays up to 12 MeV, using a linear plastic scintillating fiber array [19, 20].

This work aims at a comparative study on energy dependence of absorbed, intrinsic, photo-peak and absolute total efficiency for polystyrene (PS), polyvinyl-toluene (PVT) with NaI(Tl) scintillation detectors using Geant4 [21] version 9.6 toolkit. Subsequently, the effects of geometry parameters have been investigated. The dependence of various efficiencies has been studied by varying detector radii, thickness and geometries including cylindrical and slab cases for various source geometries and source-to-detector configurations. Normally, the response of plastic scintillation detector is a two-step process: (a) deposition of energy of incident radiations and (b) signal generation through scintillation light output. This work is focused on the simulation of energy deposition part. In the next section, the details of Geant4 (version 9.6) application development for this work are presented with underlying assumptions, overall logical flow in tracking particles and scoring methods. Thereupon, regression tests of the present simulations are presented and the results of these simulations were compared with the results collected by others. Finally new results on dependence of various detection efficiencies on the dimensions of detector, on geometry of source and on source to detector distance are presented.

MATERIALS AND METHOD

Both fibre and slab type plastic scintillators were considered in this work. The model for plastic scintillating fibre (PSF) used in Geant4 simulation is shown as fig. 1. According to the manufacturer, the scintillating material is enclosed within poly-methyl methacrylate (PMMA) cladding having thickness 0.3 % of the scintillating core diameter [22]. Selected properties of plastic materials used in this work are shown as tab. 1.

The Monte Carlo simulations were carried out using Geant4 [17, 21] version 9.6 toolkit. This toolkit is capable of particle tracking for various types of sources and it can handle different detector geometries with various types of intervening media. The Geant4 Low Energy Electromagnetic Package, based on the Livermore Data Libraries, was adopted in this work to describe photon and electrons interactions. This model includes photoelectric effect, Compton scattering, Rayleigh effect, Bremsstrahlung, and ionization processes. The threshold of production of secondary particles (cut) was chosen at 0.1 mm which is much smaller than the dimensions of the scintillator so that the energy deposition remained insensitive to the variations in cut value. Primary particles were generated independently from the cut. For each point in the graph, tracking of 10^6 photon histories was carried out in Geant4.9.6 simulations, the procedure was repeated three times and the average results were employed. The Geant4 simulation model was coded to calculate various efficiencies from the simulation results. The

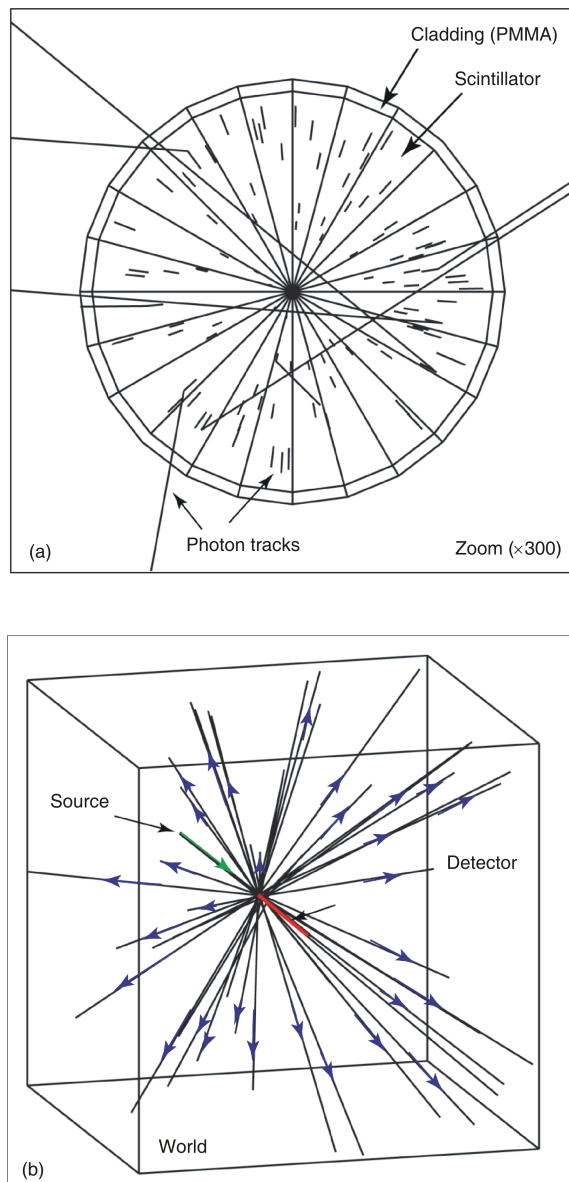


Figure 1. Geant4.9.6 generated visualization of (a) cross-section of plastic scintillation fiber and (b) incident and scattered photons with plastic scintillator

intrinsic efficiency was calculated from the ratio of gamma rays detected by detector to the gamma rays incident on the detector. Absorption efficiency was determined using the ratio of gamma rays that are fully stopped in the detector to the gamma rays that are emitted by the source. Absolute efficiency was calculated by the ratio of number of gamma rays detected to the number of gamma rays emitted by the source.

In order to compare the predictions of Geant4.9.6 with the results of earlier work, a cylindrical plastic scintillator was also considered. Scintillator of 10 cm length and diameter of one mm was used. Initially the source to detector distance of 120 cm was kept in this work. To find impact of detector radius on the intrinsic efficiency of polystyrene, simulations were performed by varying detector radius from 0.1 mm to 100 mm and the fiber length was kept at the value of 10 cm. The length of plastic scintillating fibre (PSF) is another important parameter that has effect on the intrinsic efficiency of plastic scintillator. Too small length of these scintillators leads to partial deposition of energy. Therefore simulations were carried out to find impact of fiber length on intrinsic efficiency of PS varying it from zero to 20 cm in steps and at each step the intrinsic efficiency was determined.

RESULTS AND DISCUSSION

Cylindrical scintillator geometry

In the first part of this work, using cylindrical scintillators, the simulations for cylindrical plastic scintillators were done at different energies. The values of intrinsic efficiency of polystyrene were compared with the corresponding data found by using Geant4.8.1 [19, 20]. These comparisons are shown as a function of energy in fig. 2. Good agreements are observed throughout the energy range and maximum deviation in all results remained less than 4%. A similar agreement is also observed in the comparison of the computed variation of intrinsic efficiency of PSF of the length of 10 cm and 0.25 mm diameter using Geant4.9.6 with the corre-

Table 1. Important properties of plastic scintillators used in Geant4 simulations

Property	BCF-20	BC-400	NaI(Tl)
Detector base	PS	PVT	Sodium iodide
Chemical composition	C_8H_8	$C_{10}H_{11}$	NaI(Tl)
Density [gcm^{-3}]	1.05	1.032	3.67
Refractive index	1.6	1.58	1.85
Emission color	Green	Blue	Indigo
Emission peak [nm]	492	423	415
Decay time [ns]	2.7	2.4	250
Attenuation length [m]	>3.5	1.6	0.028
Number of photons per MeV	~8000	~10000	~40000
Characteristics/applications	Fast green	General purpose	General purpose
Operating temperature	-20 °C to +50 °C	-60 °C to +20 °C	-
Ratio of H:C atoms	~1.006	~1.103	-

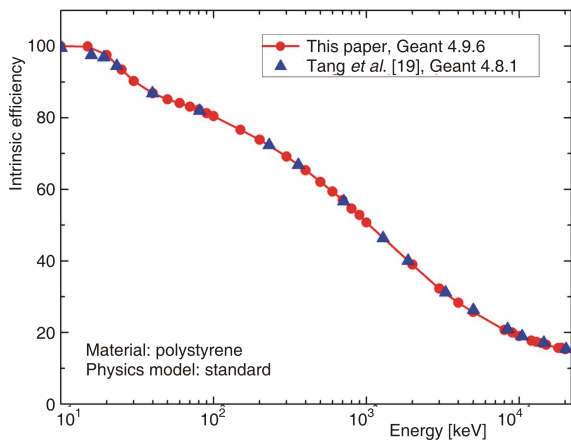


Figure 2. Comparison of energy dependence of intrinsic efficiency of polystyrene with the results of Tang *et al.*, [19]

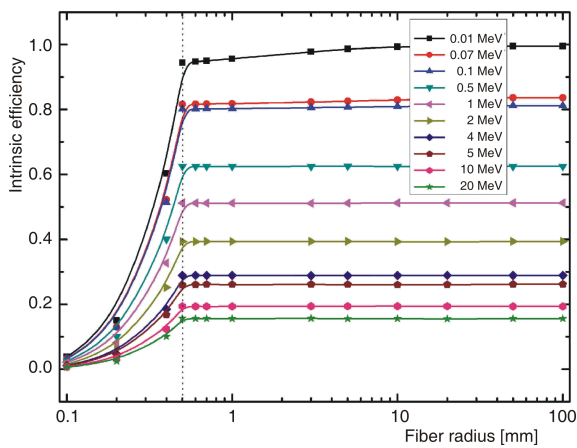


Figure 3. Variation of intrinsic total efficiency of polystyrene with fiber radius for various incident photon energies

sponding results obtained using Geant4.5.1. Good agreement is seen between the two corresponding sets of data with the maximum deviation value of 5 % throughout the 1 keV-20 MeV energy range.

Then, dependence of efficiency on PSF on radius for cylindrical systems was determined keeping the length at 10 cm. The simulation results are shown in fig. 3. Consistent with the expected behavior, the value of intrinsic efficiency increases in quadratic manner with increase in the detector radius when the detector radius is smaller than the incident photon beam radius; and beyond it, the value of efficiency becomes nearly constant. This behavior is observed over a wide variation of incident photon energies ranging from 0.01 MeV-20 MeV (fig. 3). For high energy (~20 MeV) photons, the curve beyond 0.5 mm radius shows slight variation as it approaches saturation value. This may be attributed to energy leakage effect due to secondary particles that are eventually trapped with increasing values of scintillator radii.

As a next step, the effect of plastic scintillator fiber length on efficiency was determined at different energies and results of Geant4 simulations are shown in fig. 4. The value of intrinsic efficiency rises non-linearly from low values to saturation values when the plastic scintillator fiber length is increased. For low values of incident photon energies (~0.01 MeV), the rise of efficiency to saturation values is sharp, requiring only about 2.5 cm scintillator length to reach the maximum value. This is due to large value of scintillator attenuation coefficient for these values of photon energy which leads to fast attenuation in relatively short penetration depths of plastic fibers. However, when energy of photons is high, the rise is slow and maximum value of intrinsic efficiency becomes low.

Plastic scintillation detectors are generally believed to be effective in the low energy range of incident photons. In order to study the variation of photo-peak efficiency of polystyrene with photon energy, Geant4.9.6 simulations have been performed and comparison of these results with the corresponding data obtained with Geant4.8.1 is shown in fig. 5 [19]. The Geant4.9.6 simulated results are in good agreement with the corresponding results obtained by Geant4.8.1 and maximum deviation remained less than 3-4%. These results were also compared with efficiencies obtained for PVT over the same energy range using Geant4.9.6. The PS and PVT show nearly identical behavior for the variation of photo-peak efficiency with energy. It was observed in this work that the value of photo-peak efficiency drops rapidly from nearly 100 % at 10 keV to ~1 % near 70 keV.

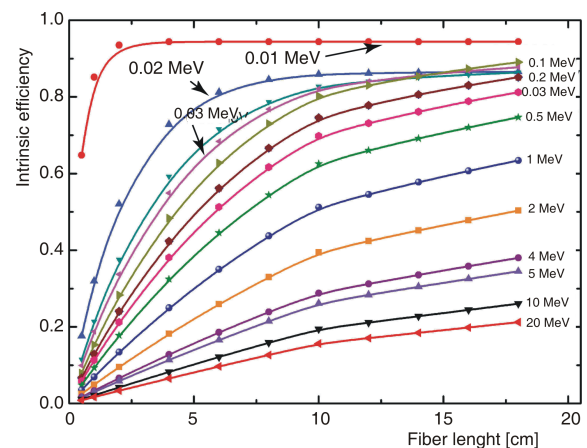


Figure 4. Variation of intrinsic total efficiency of polystyrene with fiber length for different values of photon energies

Comparison of plastic scintillators with NaI(Tl)

The PVT scintillators are widely used in portal monitors especially when large sizes of detectors are involved. While PVT is good for gross counting, it

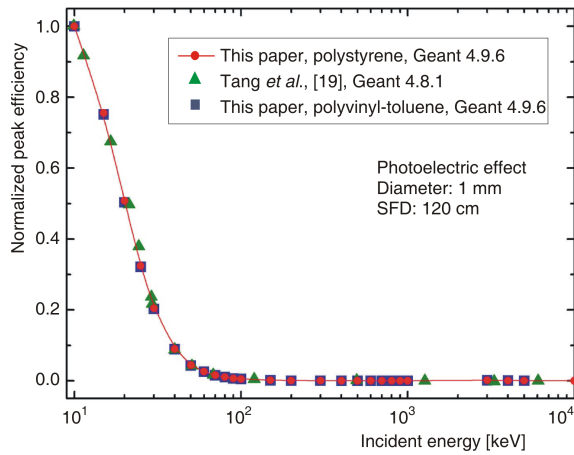


Figure 5. Dependence of the normalized peak efficiency on photon energy and comparison with results obtained by Tang *et al.*, for polystyrene [19]

performs poorly at isotope identification [23]. For this purpose, alternate available scintillators are compared against PVT for their evaluation. In this study, the values of absolute total efficiency of PS and NaI(Tl) obtained using Geant4.9.6 have been compared with that of PVT for various values of detector radius. These re-

sults are shown in tab. 2. The Geant4.9.6 results for NaI(Tl) are in excellent agreement with the corresponding data obtained by using MCNP code (Ayaz-Maierhafer and DeVol, 2007) and maximum absolute deviation remains within 1.94 %. when NaI(Tl) is compared with PS scintillator, the absolute total efficiency values for PS scintillators are only 0.367 and 0.360 times the corresponding values of NaI(Tl) for 2.54 cm and 7.62 cm detector diameters, respectively.

The values of absolute peak efficiency of PS and NaI(Tl) were also compared with that of PVT for detectors diameter values of 2.54 and 7.62 cm using Co-60 (1332 keV γ -rays) in Geant4.9.6. Results obtained by using MCNP code [23] are also compared and are shown in tab. 3. These results remained in good agreement with each other and maximum absolute deviation remained less than 2.72 %.

The dependence of absolute total detection efficiency on the γ -ray energy for NaI(Tl) and PVT was studied using Geant4.9.6 and the corresponding results are given as tab. 4. These are for point isotropic source placed at 25 cm and 100 cm from detector respectively. When we compare the corresponding values computed by Ayaz-Maierhafer and DeVol using

Table 2. Simulated results for absolute total efficiency having various diameters and thicknesses

Detector	Thickness [cm]	Diameter [cm]	Absolute total efficiency*	Absolute total efficiency (this paper)	Relative efficiency	Relative efficiency (this paper)
PVT**	–	–	$9.19 \cdot 10^{-2}$	–	1	1
NaI:Tl	1	2.54	$1.03 \cdot 10^{-4}$	$1.01 \cdot 10^{-4}$	0.001	0.001
PS	1	2.54	–	$3.71 \cdot 10^{-5}$	–	0.0004
NaI:Tl	1	7.62	$9.19 \cdot 10^{-4}$	$9.19 \cdot 10^{-4}$	0.01	0.01
PS	1	7.62	–	$3.31 \cdot 10^{-4}$	–	0.0036
NaI:Tl	1	12.7	$2.5 \cdot 10^{-3}$	$2.48 \cdot 10^{-3}$	0.027	0.027
PS	1	12.7	–	$9.04 \cdot 10^{-4}$	–	0.009
NaI:Tl	1	100	$6.28 \cdot 10^{-2}$	$6.28 \cdot 10^{-2}$	0.683	0.683
PS	1	100	–	$2.34 \cdot 10^{-2}$	–	0.2546
NaI:Tl	2.5	2.54	$2.15 \cdot 10^{-4}$	$2.14 \cdot 10^{-4}$	0.002	0.002
PS	2.5	2.54	–	$8.42 \cdot 10^{-5}$	–	0.0009
NaI:Tl	2.5	7.62	$1.91 \cdot 10^{-3}$	$1.92 \cdot 10^{-3}$	0.021	0.0209
PS	2.5	7.62	–	$7.49 \cdot 10^{-4}$	–	0.0081
NaI:Tl	2.5	12.7	$5.19 \cdot 10^{-3}$	$5.19 \cdot 10^{-3}$	0.056	0.056
PS	2.5	12.7	–	$2.04 \cdot 10^{-3}$	–	0.022
NaI:Tl	2.5	100	$1.26 \cdot 10^{-1}$	$1.27 \cdot 10^{-1}$	1.373	1.3802
PS	2.5	100	–	$5.29 \cdot 10^{-2}$	–	0.5756
NaI:Tl	7.62	2.54	$3.96 \cdot 10^{-4}$	$3.92 \cdot 10^{-4}$	0.0043	0.0042
PS	7.62	2.54	–	$1.89 \cdot 10^{-4}$	–	0.00205
NaI:Tl	7.62	7.62	$3.49 \cdot 10^{-3}$	$349 \cdot 10^{-3}$	0.038	0.038
PS	7.62	7.62	–	$1.69 \cdot 10^{-3}$	–	0.0183
NaI:Tl	7.62	12.7	$9.46 \cdot 10^{-3}$	$9.52 \cdot 10^{-3}$	0.103	0.1036
PS	7.62	12.7	–	$4.62 \cdot 10^{-3}$	–	0.0502
NaI:Tl	7.62	100	$2.19 \cdot 10^{-1}$	$2.21 \cdot 10^{-1}$	2.38	2.4039
PS	7.62	100	–	$1.21 \cdot 10^{-1}$	–	1.3166

*Ayaz-Maierhafer *et al.* [23]; **Dimensions of PVT detector: 18.88 cm 60.96 cm 5.08 cm

Table 3. Simulated results for absolute peak efficiency at 1332 keV having various diameters & thicknesses

Detector	Thickness [cm]	Diameter [cm]	Absolute peak efficiency*	Absolute peak efficiency (this paper)	Relative efficiency	Relative efficiency (this paper)
PVT**	–	–	$1.13 \cdot 10^{-4}$	–	1	–
NaI:Tl	1	2.54	$1.23 \cdot 10^{-5}$	$1.21 \cdot 10^{-5}$	0.11	0.107
PS	1	2.54	–	$3.39 \cdot 10^{-7}$	–	0.003
NaI:Tl	1	7.62	$1.47 \cdot 10^{-4}$	$1.47 \cdot 10^{-4}$	1.3	1.3
PS	1	7.62	–	$7.17 \cdot 10^{-7}$	–	0.0063
NaI:Tl	1	12.7	$4.29 \cdot 10^{-4}$	$4.22 \cdot 10^{-4}$	3.8	3.73
PS	1	12.7	–	$1.93 \cdot 10^{-5}$	–	0.17
NaI:Tl	1	100	$1.22 \cdot 10^{-2}$	$1.20 \cdot 10^{-2}$	108	106.19
PS	1	100	–	$6.15 \cdot 10^{-4}$	–	5.442
NaI:Tl	2.5	2.54	$3.53 \cdot 10^{-5}$	$3.53 \cdot 10^{-5}$	0.31	0.31
PS	2.5	2.54	–	$1.34 \cdot 10^{-6}$	–	0.011
NaI:Tl	2.5	7.62	$4.94 \cdot 10^{-4}$	$4.96 \cdot 10^{-4}$	4.38	4.38
PS	2.5	7.62	–	$2.50 \cdot 10^{-5}$	–	0.2212
NaI:Tl	2.5	12.7	$1.51 \cdot 10^{-3}$	$1.52 \cdot 10^{-3}$	13.3	13.45
PS	2.5	12.7	–	$8.76 \cdot 10^{-5}$	–	0.775
NaI:Tl	2.5	100	$4.49 \cdot 10^{-2}$	$4.52 \cdot 10^{-2}$	398	400
PS	2.5	100	–	$2.74 \cdot 10^{-3}$	–	24.24
NaI:Tl	7.62	2.54	$7.89 \cdot 10^{-5}$	$7.77 \cdot 10^{-5}$	0.7	0.686
PS	7.62	2.54	–	$2.78 \cdot 10^{-6}$	–	0.024
NaI:Tl	7.62	7.62	$1.34 \cdot 10^{-3}$	$1.34 \cdot 10^{-3}$	11.9	11.9
PS	7.62	7.62	–	$7.76 \cdot 10^{-5}$	–	0.686
NaI:Tl	7.62	12.7	$4.38 \cdot 10^{-3}$	$4.41 \cdot 10^{-3}$	38.8	39.02
PS	7.62	12.7	–	$3.18 \cdot 10^{-6}$	–	0.03
NaI:Tl	7.62	100	$1.39 \cdot 10^{-1}$	$1.41 \cdot 10^{-1}$	1230	1246.79
PS	7.62	100	–	$2.03 \cdot 10^{-2}$	–	179.64

*Ayaz-Maierhafer *et al.* [23]; **Dimensions of PVT detector: 18.88 cm 60.96 cm 5.08 cm

Table 4. The comparison of simulated values of absolute total efficiency ($\epsilon_{abs,total}$) and absolute peak efficiency at 1332 keV ($\epsilon_{abs,1332\text{ keV}}$) of PVT with NaI(Tl) values using Geant 4.9.6

Source-detector distance [cm] (source)	Efficiency	PVT**	PVT (this paper)	NaI:Tl* (7.62 cm diameter 7.62 cm)	NaI:Tl (this paper) (7.62 cm diameter 7.62 cm)	NaI:Tl* (100 cm diameter 1 cm)	NaI:Tl (this paper) (100 cm diameter 1 cm)
25 (Co-60)	Absolute, total	0.0919	–	0.0379	0.0376	0.68	0.676
	Absolute, 1332 keV	0.0001	–	11.88	11.69	108.00	109.73
25 (Cs-137)	Absolute, total	0.108	–	0.0373	0.0383	0.76	0.804
	Absolute, 662 keV	0.0002	–	10.66	10.757	136.70	136.37
100 (Co-60)	Absolute, total	0.0177	–	0.0146	0.0141	0.52	0.508
	Absolute, 1332 keV	.00002	–	4.947	4.865	85.82	83.50
100 (Cs-137)	Absolute, total	–	0.0232	–	0.0126	–	0.560
	Absolute, 662 keV	–	.000041	–	4.219	–	107.80

*Ayaz-Maierhafer *et al.* [23]; **Dimensions of PVT detector: 18.88 cm 60.96 cm 5.08 cm

MCNP code, we see that Geant4.9.6 predictions are in excellent agreement with MCNP results [23] and maximum absolute deviations is less 3.65 % in all cases. With increase in the value of γ -ray energy, the values of absolute total efficiency shows decreasing trend

which is consistent with the respective decrease in the attenuation coefficient values in this energy range.

The dependence of absorption efficiency of polystyrene on incident photon energy has also been simulated using Geant4.9.6 and the results were com-

pared with the corresponding results from Geant4.8.1 [19]. Both are in good agreement as shown as fig. 6. This figure shows a sharp decreasing trend in the low energy range which can be attributed to the corresponding variation in photo-electric effect. However, when the absorption efficiency of polystyrene computed by Geant4.9.6 is compared with the corresponding data from Geant4.5.1 [24], some discrepancies are observed in the absorption efficiency values near 250 keV-300 keV energy range, and these could be attributed to the difference in the physics libraries used in two versions of Geant4 toolkits.

Leakage energy and fiber length effects

A bundle of PSF is normally used in experimental measurements and cross-talk caused by partial absorption of energy in various fibers effects the measurements. In order to study this process, the dependence of absorption efficiency on fiber length has been computed for 100 keV incident photons using Geant4.9.6 code. In fig. 7, the results for various values of fiber diameter were compared with the corresponding results obtained by Geant4.8.1 [19]. The Geant4.9.6 values of absorption efficiency are in good agreement with the results obtained by using Geant4.8.1 code. The absorption efficiency increases quickly as the fiber length increases to about 10 cm and then it continues rising with reduced slope. When fiber length is less than 4 cm, the absorbed efficiency remains independent of the fiber diameter and when fiber length becomes more than 4 cm, the larger fiber diameter exhibits a higher value of absorption efficiency. This is due to secondary particles with large transverse momentum as they get absorbed effectively in larger diameter fibers. For longer lengths, and small diameters, the cross-talk remains high due to leakage

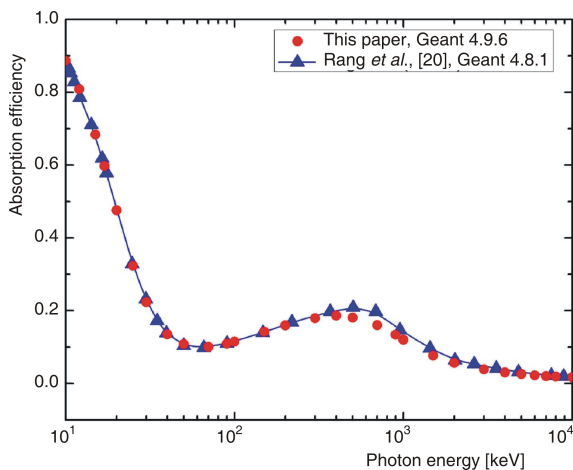


Figure 6. Variation of absorption efficiency of polystyrene with photon energy

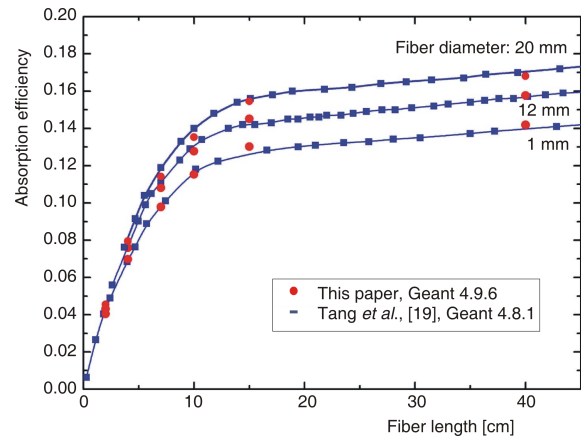


Figure 7. Dependence of absorption efficiency of polystyrene on fiber length for indicated values of fiber diameter

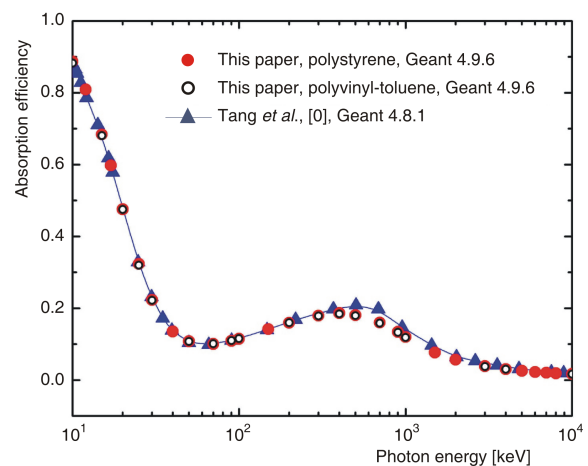


Figure 8. Energy dependence of the detection efficiency of polystyrene and polyvinyl-toluene

of secondary particles with large transverse momentum.

The absorption efficiency plays pivotal role in determination of scintillation detection efficiency which is essentially a product of the absorption efficiency, conversion efficiency and transmission efficiency. Comparison of absorption efficiency of PS with that of PVT has been carried out using Geant4.9.6. These results were compared with the work of Tang *et al.*, on variation of absorption efficiency of PS [19]. The comparison is given as fig. 8. Clearly, the three data sets are in good agreement with each other indicating radiological similarity of PVT with PS in this energy range.

Slab scintillator geometry

Recently, efforts were made to replace PVT with other types of detectors in portal monitors as PVT has a

Table 5. Comparison of simulated absolute detection efficiency of PS, PVT, and NaI(Tl) using Geant4.9.6 code

Source/(source to detector distance)	Efficiency	PVT (this paper) (188.88 × 60.96 × 5.08)	Polystyrene (this paper) (188.88 × 60.96 × 5.08)	NaI:Tl* (47 × 58.5 × 0.95)	NaI:Tl (this paper) (47 × 58.5 × 0.95)	NaI:Tl* (10.16 × 10.16 × 40.64)	NaI:Tl (this paper) (10.16 × 10.16 × 40.64)
⁶⁰ Co (25 cm)	Absolute, total	1.0237	1.0314	0.3568	0.3606	0.3096	0.3048
	Absolute, 1332 keV	1	1.0353	53.13	53.398	138.5	133.337
¹³⁷ Cs (25 cm)	Absolute, total	1.0412	1.0498	0.3993	0.4382	0.2933	0.3096
	Absolute, 662 keV	0.9282	0.9641	69.45	69.5964	103.7	109.404
⁶⁰ Co (100 cm)	Absolute, total	1.0508	1.063	0.1876	0.1807	0.1437	0.1434
	Absolute, 1332 keV	0.935	1.05	29.33	28.7	69.57	71.671
¹³⁷ Cs (100 cm)	Absolute, total	1	1.00702	–	0.2038	–	0.1253
	Absolute, 662 keV	1	1.1219	–	36.58	–	53.475

*Ayaz-Maierhafer *et al.*, [23]; **Using corresponding values for PVT as reference

Table 6. Dimensions of slabs and fibers along with corresponding surface areas

Surface area of front side	Dimensions of slab [cm]	Dimensions of fiber (diameter length)
7.85 × 10 ⁻³ cm ²	(0.088 × 0.088 × 10)	(1 mm × 10 cm)
1.1309 cm ²	(1.063 × 1.063 × 10)	(12 mm × 10 cm)
3.1415 cm ²	(1.772 × 1.772 × 10)	(20 mm × 10 cm)

drawback of requiring a second screening for isotope identification [23]. In this regard, we have compared polystyrene, PVT and NaI(Tl). First the absolute detection efficiency has been estimated for polystyrene and PVT employing Geant4.9.6 code with a point isotropic source at 25 cm and at 100 cm, respectively, from the detector. These results have been compared with the corresponding results for NaI(Tl) by Ayaz-Maierhafer and DeVol using MCNP code [23] and are shown as tab. 5. The Geant4.9.6 computed values are in reasonable agreement with the corresponding data by MCNP code with maximum relative error remained less than 9.7%. The corresponding data also show excellent agreement for absolute total efficiency values when Co-60 is used. The maximum absolute relative error remained less than 2%.

Then the effects of geometry were compared in this work. In order to quantify the effect of geometry on intrinsic efficiency of polystyrene fibers, both the slab type and cylindrical models were used in Geant4.9.6. These models had identical cross sectional area and volumes. The only difference was in the geometry. The dimensions of slab and cylindrical polystyrene scintillators are given in tab. 6. For cylindrical fibers, each fiber had a length of 10 cm and the fiber diameter was allowed to vary from one mm to 20 mm. For three different front surface areas the results of Geant4 are shown as fig. 9. The results show

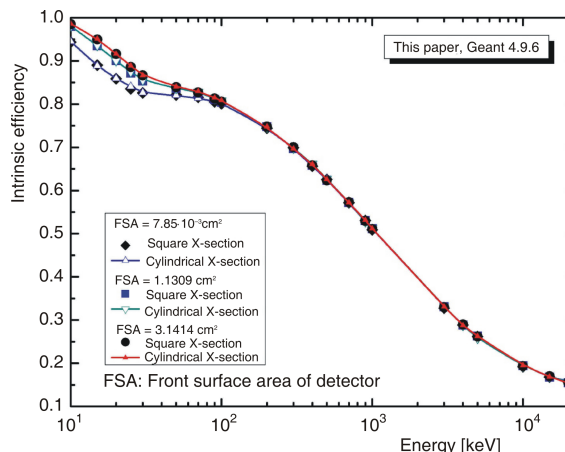


Figure 9. The intrinsic efficiency as a function of energy obtained by using Geant4.9.6 for various fiber and slab geometries

that the intrinsic efficiency that is largely independent of the geometry, and differences in the values of intrinsic efficiency between corresponding cylindrical or square cross-sectional geometries are negligible. When incident photon energy is less than 100 keV (fig. 9), the increase in cross-sectional area does not increase the intrinsic efficiency and for all energies greater than 100 keV, it is independent of cross-sectional area.

The efficiency of a scintillator is largely determined by the linear attenuation coefficient of the detector material. The variation of attenuation coefficient of polystyrene, PMMA, water, soft tissue and muscle was computed by carrying out the attenuation simulation of a parallel beam of photons of specific energy in a slab of material using Geant4.9.6. The computed values for BC-400 type of commercial polystyrene have been compared with the corresponding

values computed by MCNP code and also with reported data by manufacturer [22]. Results showed that values are in good agreement with the corresponding published data in the 0.01 MeV-10 MeV energy range. Also, BC-400 has approximately the same values of μ as soft tissues have for the same energy range.

CONCLUSIONS

In this work, comparative study of energy dependence of absorbed, intrinsic, photo-peak and absolute total efficiency of PSF and PVT detectors was done with NaI(Tl) scintillation detectors using Geant4 version 9.6 toolkit. The effects of geometry parameters on various efficiencies were studied by varying detector radii, thickness and various source-to-detector configurations. This work confirms that plastic scintillator based fiber and slab detectors are suitable for X-ray and low energy γ -ray applications with energies typically below 50 keV, including counting and medical and industrial radiographic imaging purposes. The optimum length of PSF has been confirmed as 10 cm. For high energy range, cross talk is an issue for PSF which is expected to be more prominent in fibers of longer lengths and of small diameter values. The detector intrinsic efficiency shows increasing behavior with radius while the radius remains smaller than incident photon beam radius and beyond it, the efficiency becomes constant.

AUTHOR CONTRIBUTIONS

Main idea of this work was developed by S. M. Mirza and N. M. Mirza. The actual research work on GEANT4 was carried out by A. Razzaq and then comparisons with other studies were done by S. Ur Rehman. The paper text was written by N. M. Mirza. The paper figures were drawn by S. M. Mirza and A. Razzaq. The tables were prepared by A. Razzaq with S. Ur Rehman.

REFERENCES

- [1] Beddar, A. S., Plastic Scintillation Dosimetry and Its Application to Radiotherapy, *Radiation Measurements*, 41 (2007), pp. S124-S133
- [2] Toh, K., et al., Radiation-Resistant Optical Fiber/Scintillator System for Gamma-Ray Monitor, *Nuclear Instruments and Methods in Physics Research Section A: Accelerators, Spectrometers, Detectors and Associated Equipment*, 700 (2013), pp. 130-134
- [3] Eriksson, L. A., et al., Comparative Studies on Plastic Scintillators – Applications to Low Energy High Rate Photon Detection, *Nuclear Instruments and Methods*, 122 (1974), 1, pp. 373-376
- [4] White, T., Scintillating Fibers, *Nuclear Instruments and Methods*, 273 (1988), 2-3, pp. 820-825
- [5] Clark, D., The Intrinsic Scintillation Efficiency of Plastic Scintillators for ^{60}Co Gamma Excitation, *Nuclear Instruments and Methods*, 117 (1974), 1, pp. 295-303
- [6] Shao, H., Miller, D. W., Pearsall, C. R., Scintillating Fiber Optics for X-Ray Radiation Imaging, *Nuclear Instruments and Methods – A*, 299 (1990), 1-3, pp. 528-533
- [7] Imai, S., et al., New Radiation Detector of Plastic Scintillation Fiber, *Rev. Sci. Instrum.*, 62 (1991), pp. 1093-1097
- [8] Beddar, A. S., Mackie, T. R., Attix, F. H., Water-Equivalent Plastic Scintillation Detectors for High Energy Beam Dosimetry: Properties and Measurements, *Phys. Med. Biol.*, 37 (1992), 10, pp. 1901-1913
- [9] Mainardi, R. T., Bonzi, E. V., Monte Carlo Calculation of Radiation Energy Absorbed in Plastic Scintillators, *Radiation Physics and Chemistry*, 45 (1995), 5, pp. 691-693
- [10] Aoyama, T., et al., A Depth-Dose Measuring Device Using a Multichannel Scintillating Fiber Array for Electron Beam Therapy, *Medical Physics*, 24 (1997), 8, pp. 1235-1239
- [11] Kirov, A. S., et al., Towards Two-Dimensional Brachytherapy Dosimetry Using Plastic Scintillator: New Highly Efficient Water Equivalent Plastic Scintillator Materials, *Medical Physics*, 26 (1999), 8, p. 1515
- [12] Lambert, J., et al., A Plastic Scintillation Dosimeter for High Dose Rate Brachytherapy, *Phys. Med. Biol.*, 51 (2006), 21, pp. 5505-5516
- [13] Briesmeister, J. F., MCNP-A General Monte Carlo Code for Neutron and Photon Transport, LA-7396-M, Los Alamos National Laboratory, N. Mex., USA, 1986
- [14] Nasser, M. M., et al., X-Ray Imaging Using a Single Plastic Scintillating Fiber, *Nuclear Instruments and Methods in Physics Research Section B: Beam Interactions with Materials and Atoms*, 225 (2004), 4, pp. 617-622
- [15] Alcon, E. P., Lopes, R. T., de Almeida, C. E., EPR Study of Radiation Stability of Organic Plastic Scintillator for Cardiovascular Brachytherapy Sr90-Y90 Beta Dosimetry, *Applied Radiation & Isotopes* 62 (2005), 2, pp. 301-306
- [16] Baro, J., et al., PENELOPE: An Algorithm for Monte Carlo Simulation of the Penetration and Energy Loss of Electrons and Positrons in Matter, *Nuclear Instruments and Methods in Physics Research Section B: Beam Interactions with Materials and Atoms*, 100 (1995), pp. 31-46
- [17] Agostinelli, S., et al., Geant4-a Simulation Toolkit, *Nuclear Instruments and Methods in Physics Research Section A: Accelerators, Spectrometers, Detectors and Associated Equipment*, 506 (2003), 3, pp. 250-303
- [18] Nasser, M. M., et al., Low Energy X-Ray Imaging Using Plastic Scintillating Fiber: A Simulation Study, *Nuclear Instruments and Methods in Physics Research Section B: Beam Interactions with Materials and Atoms*, 234 (2005), 3, pp. 362-368
- [19] Tang, S.-B., et al., Simulation Study of Energy Absorption of X and γ -Rays in Plastic Scintillating Fiber Arrays, *IEEE Transactions on Nuclear Science*, 54 (2007), 5, pp. 1773-1778
- [20] Tang, S.-B., et al., Simulation Study on Detection Efficiency of Plastic Scintillating Fiber Under γ -Ray Radiation, *Radiation Physics and Chemistry* 77 (2008), 2, pp. 115-120
- [21] Allison, J., et al., The Geant4 Visualization System, *Computer Physics Communications*, 178 (2008), pp. 331-365
- [22] ***, BICRON, Scintillation Products: Scintillating Optical Fibers, in: *Saint-Gobian Crystals*, Hiram, O., USA, 2005

- [23] Ayaz-Maierhafer, B., DeVol, T. A., Determination of Absolute Detection Efficiencies for Detectors of Interest in Homeland Security, *Nuclear Instruments and Methods in Physics Research Section A: Accelerators, Spectrometers, Detectors and Associated Equipment* 579 (2007), 1, pp. 410-413
- [24] Nasser, M. M., Qingli, M., Zejie, Y., Sensitivity of Plastic Scintillating Fiber Optic for X- and γ -Radia-

tion, a Simulation Study, *Sensors and Actuators A: Physical*, 122 (2005), 1, pp. 64-67

Received on June 23, 2015

Accepted on September 28, 2015

Сикандер М. МИРЗА, Ахсан РАЗАК, Шакил Ур РЕХМАН, Насир М. МИРЗА

**ПРОУЧАВАЊЕ УТИЦАЈА РАЗЛИЧИТИХ ГЕОМЕТРИЈА НА ЕФИКАСНОСТ
ДЕТЕКЦИЈЕ ПОЛИСТИРЕНСКИХ, ПОЛИВИНИЛ ТОЛУЕНСКИХ И
НАТРИЈУМЈОДИДНИХ ДЕТЕКТОРА ПОМОЋУ КОДА GEANT4**

У овом раду приказано је компаративно проучавање енергетске зависности апсорбоване, сопствене, фотопике апсолутне укупне ефикасности полистиренских пластичних сцинтилаторских влакана и поливинил толуенских детектора са NaI(Tl) сцинтилационим детекторима, обављено употребом Geant4 софтверског алата верзије 9.6. Променом полупречника и дебљине детектора, као и растојања извор–детектор, испитани су утицаји геометријских параметара на различите ефикасности. Ова испитивања обављена су за цилиндричне и плочасте геометрије и са фотонима енергија од 10 keV до 20 MeV, коришћењем тачкастих изотропних извора и паралелних снопова фотона. Поређење резултата симулације полистиренских пластичних сцинтилаторских влакана обављених кодом Geant 4.9.6, са одговарајућим резултатима добијеним кодовима Geant4 (верзија 5.1) и Geant4 (верзија 8.1), показују добро слагање зависности сопствене ефикасности од енергије фотона. Добро слагање са објављеним резултатима уочено је и за варијацију сопствене ефикасности у функцији енергије фотона код поливинил толуенских детектора. Овај рад потврђује да су влакна заснована на пластичним сцинтилаторима и плочасти детектори погодни за примену код X-зрачења и нискоенергетског гама зрачења са енергијама типично испод 50 keV и оптималном дужином влакана од 10 cm. За опсеге високих енергија, преслушавање остаје проблем за полистиренска пластична сцинтилаторска влакна и истакнут је код влакана која имају велике дужине и мале пречнике. Такође, све док је полупречник влакна мањи од инцидентног снопа фотона, сопствена ефикасност влакна расте са повећањем полупречника.

Кључне речи: пластично сцинтилаторско влакно, поливинил толуенски сцинтилатор, ефикасност детекције, Geant4